SKELETAL ANOMALIES IN SENEGALESE SOLE (*SOLEA SENEGALENSIS*), AN ANOSTEOCYTIC BONED FLATFISH SPECIES

AM de Azevedo[1], AP Losada[1], A Barreiro[1,2], S. Vázquez[1] and M.I. Quiroga[1]

[1]Departamento de Anatomía, Producción Animal y Ciencias Clínicas Veterinarias, Facultade de Veterinaria, Universidade de Santiago de Compostela. Lugo, Spain.

[2]Hospital Veterinario Universitario Rof Codina. Lugo, Spain

Corresponding author: Ana M. de Azevedo, Departamento de Anatomía, Producción Animal y Ciencias Clínicas Veterinarias, Facultade de Veterinaria, Universidade de Santiago de Compostela, Campus Universitario s/n, Lugo 27002, Spain. Telf. +34 982 822 306. E-mail: anazevedogomes@hotmail.com

Abstract

Skeletal anomalies affect animal welfare and cause important economic problems in aquaculture. Despite the high frequency of skeletal problems in reared *Solea senegalensis*, there is lack of information regarding the histological features of normal and deformed vertebrae in this flatfish. The aim of this study was to describe the histopathological and radiographical appearance of vertebral body anomalies. Sixty-seven juvenile fish were radiographically examined 104 or 105 days after hatching. Through radiographic images, vertebral segments were selected and processed for histopathological examination from seven normal and seven affected fish. Alterations in bone shape and vertebral fusion were the most significant anomalies in the vertebral bodies. These alterations occurred most frequently between the last three abdominal vertebrae and the first ten caudal centra. Radiographically, deformed vertebrae showed flattening of the endplates and narrowing of the intervertebral spaces. The radiographic findings concurred with the histological lesions where affected vertebrae exhibited irregular endplates and changes in trabecular bone. Radiolucent cartilaginous tissue was evident in the endplates of the deformed vertebra and, in some cases, the cartilaginous material extended from the growth zone into the intervertebral space. These changes were likely the primary alterations that lead to vertebral fusion. Fused vertebrae were often reshaped and showed a reorganization of the trabeculae. The formation of metaplastic cartilage is frequent in a variety of anomalies affecting teleost species.

Keywords: Anosteocytic bone, fish, histopathology, Senegalese sole (*Solea senegalensis*), skeletal anomalies, vertebrae.

Skeletal anomalies constitute a significant problem in many cultured fish,[2] and Senegalese sole (*Solea senegalensis*) are no exception.[26] Since this flatfish species has high economic value, the production in Europe has almost doubled in just one year.[12] However, this cultured fish is highly susceptible to vertebral abnormalities both in natural and in experimental conditions.[20] Some studies indicate that 44-100% of fish have deformities in some lots,[16, 19, 20] and in some fish farms the frequency of deformities reaches 80% to 100% of the fish.[7, 8, 32] Like in other fish species, these skeletal problems not only have animal welfare implications but also lead to severe economic losses as it decreases the market value and downgrades the final product.[2, 14, 25]

Skeletal deformities in Senegalese sole have been associated with various causative factors, especially those involving environmental and nutritional conditions.[1, 10, 13, 16, 35, 37] However, there is a paucity of information regarding the underlying mechanisms involved in skeletal deformities in commercial fish farming where multilevel factors interact during development.[3]

Detection of malformations is primarily done by gross examination and palpation of the fish in Senegalese sole farms,[38] and to a lesser extent by refined techniques such as double staining technique,[8, 19, 21] computed radiography,[7, 32] and even computed tomography,[31] as in other fish species.[11, 24, 42]

Laboratory tools such as histopathology and molecular biology have been used to assess vertebral anomalies in Atlantic salmon (*Salmo salar*), an osteocytic bone species.[30, 41, 47, 48, 49] The morphological and mechanical properties of anosteocytic bone (i.e. bone without osteocytes) in fish are incompletely

understood.[9] Studies in gilthead seabream (*Sparus aurata*) and European seabass (*Dicentrarchus labrax*) showed some of the histopathological alterations in vertebrae.[15, 28, 33] However, scarce reports exist on the histological features of Senegalese sole bone.[4, 5]

The aim of this work was to evaluate and correlate the radiographic and histologic changes in the vertebrae of normal and deformed juvenile Senegalese sole.

Materials and methods

A total of 67 juvenile Senegalese sole, 104 or 105 days after hatching, and ranging from 5.9 cm to 9.8 cm (standard length) were used for this study. The animals came from a fish farm located in the Northwest of Spain with a prevalence of skeletal anomalies around 40% at grading point. Fish were euthanized with an overdose of Tricaine methanesulfonate (MS-222, Sigma-Aldrich) and fixed in 10% buffered formalin. Computed radiography was performed in fixed fish placed in two orthogonal projections according to previous reports[7, 32] and using methacrylate plates to position the fish. Radiographic images were evaluated with a software program (RadiAnt DICOM Viewer 1.9.16.7446) to detect skeletal deformities. The assessment was focused exclusively on vertebral body anomalies (fusions or deformations) and spinal deviations (kyphosis, lordosis and scoliosis). The study included seven fish with radiographical evidence of vertebral deformities, and seven fish without evidence of vertebral deformity (control group). Vertebral segments containing the affected bone were trimmed, as well as the same anatomical areas for the control fish. The tissues were decalcified for 48 h in Osteodec® (Bio-Optica,

Milano, Italy) and embedded in paraffin. Parasagittal sections of tissue were cut at 3 μm and stained with hematoxylin-eosin (HE) for routine histopathological examination. For the identification of acidic mucins and cartilage, tissue sections were stained with alcian blue/hematoxylin-eosin (AB-HE) and alcian blue/periodic acid-Schiff (AB-PAS). Also, Gallego's trichrome (GT) stain was used to differentiate collagen fibers, muscle and cartilage.[34] Finally, osteoid, mature bone and cartilage were identified using a previously described modified tetrachrome osteoid stain (OS).[36] Slides were mounted using Coverquick 2000 mounting medium (Prolabo®) and observed with an Olympus® BX51 microscope with a digital camera Olympus® DP72. A comparative study was done by reviewing deformed and non-deformed vertebrae in the same fish, as well as with the corresponding segments of the control animals.

The data analyzed in this study are not available as Supplemental Materials.

Results

The radiographic approach used in juveniles allowed the detailed assessment of the vertebral column, although in the smaller fish, the definition of the caudal-most vertebral bodies (preurals and urostyle) was impaired. Radiographic images of control fish showed an aligned rachis, composed of succeeding vertebrae along the abdominal, caudal, and caudal complex region (Figs. 1a, b). The vertebrae showed an X-shape internal structure separated by radiolucent intervertebral spaces (IVS) (Fig. 2). Histologically, vertebral bodies showed a symmetrical amphicoelous form and followed a line interposed by IVS filled with the notochord (Fig. 3). Supplemental Table S1 shows the characteristics colors of the vertebral structures using different stains. Vertebrae composed of

anosteocytic osseous tissue had trabecular bone between the two endplates of laminar bone (Figs. 3, 4). A layer of osteoid-secreting osteoblasts was observed in the growth zone of the endplates covered by external intervertebral connective tissue (Fig. 4). In the IVS, the notochord was composed of vacuolated chordocytes in the center and chordoblasts in the notochordal epithelial layer (Fig. 4). Depending on the parasagittal section some chordocytes appeared less vacuolated in a denser area in the notochord centre (Fig. 3). Notochordal cells were encased in a collagenous layer (notochordal sheath) and the external elastic membrane (Fig. 4). OS revealed mature bone in the vertebral centrum, except for the endplates where osteoid was the dominant component (Fig. 5).

Spinal anomalies were found radiographically present in 7/67 (~10%) of the fish. Vertebral deformation and fusion were the two major anomalies, affecting 6/7 and 3/7 of the selected fish, respectively. These lesions were most frequently located between the last three abdominal vertebrae (A7-9) and the first ten caudal centra (C1-10). The most common radiographic features in the deformed vertebrae were flattened and irregular endplates which often appeared more radiodense than those in the adjacent vertebrae (Fig. 6). Overall, the IVS was narrow (Fig. 6) and sometimes with an irregular outline. Microscopic alterations in the endplate paralleled those changes observed radiographically. The deformed vertebral bodies also showed alterations of the osseous internal trabeculae. The main longitudinal trabeculae were oblique, sometimes symmetrically, resembling a concave or convex (Fig. 7) structure. In 16/23 (~70%) of the deformed vertebrae, a variable number of cells resembling chondrocytes were present in the endplates, towards the IVS. These cells were

particularly prevalent in the dorsal or ventral aspect of the endplate, near the growth zone. Usually, when opposed centra trabeculae formed a convex structure, chondrocytes were located ventrally (Fig. 7). Some vertebrae had large numbers of chondrocytes separated by abundant extracellular cartilaginous matrix (ECM). The chondrocytes resided inside lacunae and were surrounded by a halo of ECM (Fig. 8).

In one sided compressions, the radiographic image of the centrum presented a "K"-like shape (Fig. 9), which microscopically corresponded with a flattened endplate from one side and oblique trabeculae (Fig. 10). In addition to the growth zone, chondrocytes were observed in the articular bone. Occasionally, aggregates of chondrocytes formed protuberances which protruded bilaterally and symmetrically towards the notochord in the IVS (Fig. 10 and inset). In 2/6 deformed fish, these protuberances joined together, forming a bridge among the vertebral bodies (Fig. 11). The thickness and height of some vertebral bodies were increased compared to the normal adjacent vertebrae (Fig. 12). Microscopically, cartilaginous tissue was invading the IVS in 2/6 fish (Fig. 13). The extension of this material ranged from 30% to 100% of the IVS, depending on the depth of the section, apparently pushing the notochord (Fig. 13).

Almost all the trabecular and articular lesions showed a mirror-image involving two consecutive vertebrae. When the affected area had only a few chondrocytes, these cells were isolated and embedded in a bone matrix, often forming a tissue compatible with chondroid (Fig. 14). Deeper into the endplate, the chondrocytes appeared smaller (Fig. 14).

More severe anomalies were observed, combining fusions and deformations (Fig. 15). These vertebrae had excessive cartilaginous tissue between fused vertebrae and the opposing centra in histological sections (Fig. 16a). However, in a serial section, chondrocytes disappeared and the IVS was occupied by notochordal structures with a small amount of ECM (Fig. 16b) related to the presence of chondrocytes in the endplate.

Cartilaginous tissue within the IVS was rich in chondrocytes surrounded by abundant ECM (Figs. 17, 18), compatible with cell-rich hyaline cartilage. Chondrocytes had different degrees of maturation depending on their location in the IVS (Fig. 17). The tissue was composed of a central area occupied with small slightly elongated chondrocytes (Figs. 17, 18). At both sides of this area, there were rounded and hypertrophied chondrocytes and a zone where cartilaginous tissue was associated with the endplates (Fig. 17, 18). In the former region, the matrix involving some groups of chondrocytes changed its affinity for the dye (Figs. 17-19). Occasionally, it was difficult to distinguish the boundaries between the cartilage in the IVS and the endplate as both looked alike.

Deformed vertebral segments also showed alterations in notochordal structures. The external elastic membrane was usually scattered and irregular in the converging area of two endplates showing chondrocytes (dorsally or ventrally) (Figs. 11, 14, 17). The collagenous layer associated with the damaged membrane was occasionally less evident or thinner (Figs. 11, 17). A high number of blood capillaries were sporadically present in the connective tissue, externally to the layer of osteoblasts (Fig. 19). A schematic summary of the

histological features in control and deformed vertebrae are illustrated in Figs. 20 and 21.

Fused vertebrae were radiographically recognized by the presence of extra neural and haemal elements (Fig. 22). In many cases, the union was reshaped, showing almost the same length as any normal vertebra (Fig. 22). Histopathologic findings in fused vertebrae consisted of the reorganization of the internal longitudinal trabeculae, but the fusion line persisted (Fig. 23a). In serial sections, remnants of the notochord and the external elastic membrane were detected in the center of the anomaly (Fig. 23a inset). In one case, a small portion of cartilaginous tissue was observed in a similar location (Fig. 16b inset). OS stain revealed mature bone in the central region of most of the fused vertebrae (Fig. 23b). Fusion involving three vertebral bodies were also detected (Fig. 24), showing two small notochord portions in the corresponding location of the former IVS (Fig. 25).

Discussion

The present study shows the most common vertebral body anomalies affecting Senegalese sole applying radiographic and histopathologic methods. As far as we know, this is the first histopathologic description of fused and deformed vertebrae unrelated with axis deviations, in this flatfish species.

The radiographic study revealed that deformations and fusions are the two major types of vertebral body abnormalities in juvenile Senegalese sole. Similar anomalies were previously described in the caudal complex vertebrae of larvae, using double staining technique for cartilage and bone, with prevalence of 19% and 25%, respectively.[8, 20] As reported in several fish species,[5, 30, 33, 41]

Senegalese sole also develop vertebral deformation with alterations of longitudinal bony trabeculae and flattened endplates. Microscopically, the deformed vertebral centra display cartilaginous alterations in the endplates and IVS, but these alterations are not evident in the radiographic images. The symmetrical characteristics of these abnormalities may indicate that the vertebral lesions likely start in the region comprising intervertebral tissue and opposing endplates.[30] In *curveback* lineage of guppies (*Poecilia reticulata*), vertebral deformations have been primarily described in the concave side of lordotic and kyphotic vertebrae.[22] This study also showed that the chondrocytes were present in the concave aspect of centra displaying an oblique symmetric orientation of the trabecular bone. Fused centra were radiographically detected by the presence of extranumerary neural and haemal structures. Also, microscopic findings suggest that trabecular remodeling or modeling occur and remnants of intervertebral notochord persisted in the fusion center. In one fish, a cartilaginous residue was found in the fusion line (just in the intersection of perpendicular trabeculae), corresponding to the location of the IVS. Similar findings were observed in Atlantic salmon intermediate and final stages of fusion.[47, 49]

The formation of cartilage constituents can be present in both anomaly types, deformations and fusions, and in distinct fish species.[4, 41, 47] These may constitute an ongoing process of aggravation of the lesions in which some deformed segments could be already showing early signs of fusion.[18, 47] Also, two fused centra showed cartilage in the adjacent IVS, indicating the progression into a three-vertebrae fusion.[47] It has been suggested that adjacent asymmetrically compressed vertebrae would fuse, while homogenously

compressed vertebrae might represent a more "stable alteration".[40, 41, 42, 47] Therefore, it would be interesting to evaluate vertebral anomaly signaling pathways as well as environmental factors involved in the containment and aggravation of the problem.[47]

The development of chondroid and cartilaginous tissue observed in skeletal anomalies is not well understood in fish. Anosteocytic teleost bone is able to perform adaptive, plastic responses to loading conditions.[9, 28, 29] The presence of cartilaginous tissue could attenuate mechanical stress at the autocentrum.[5] Also, chondroid tissue seems to meet the demand for an accelerated local growth rate and the need for a shear-resistant support.[27, 33]

Chondrocytes were located in the endplates, as reported in other studies,[5, 28, 30, 33, 41] especially near the growth zones constituted by osteoblasts and mesenchymal cells. This distribution can be based on the availability of oxygen and nutrients in the peripheral areas.[5] Our results showed the proliferation of exuberant cartilaginous tissue visibly from the growth zones into the IVS. These findings may indicate that chondrocytes could arise from metaplastic mesenchymal cells in the growth plate,[5] as a result of altered mechanical load, such as suggested for vertebral curvatures.[4] Mesenchyme cells may differentiate into chondroblasts rather than osteoblasts in response to high rates of change in compression[23] or in a low oxygen environment during fracture repair.[6] Although co-transcription of some osteogenic and chondrogenic markers may occur in the osteoblasts in the growth zone during fusion process,[49] the mesenchymal source of osteoprogenitor cells has not been clearly identified in fish.[46] Moreover, osteogenic cells can transform into osteocytes or into chondrocytes in the Atlantic salmon kype skeleton as they

become entrapped in the bone matrix.[43] Therefore, the possible involvement of osteoblasts should not be disregarded, nor the metaplastic transformation of the notochord area into cartilage.[41]

Some authors hypothesized that once the chondrocytes differentiate in the growth zone, they can be entrapped by the newly deposited osteoid matrix and eventually die due to lack of nutrients and hypoxia, with only those near the endplate surviving.[5] Another hypothesis is that cartilage could be developing into the IVS, stuck on the endplate, causing alterations in the endplate shape and compressing the notochord. The previously described hypotheses are not mutually exclusive and might represent one same subsequent process whereby cartilage is replaced by osseous tissue, as occurring in later steps of fusion.[47]

Three main mechanisms of bone formation have been described in teleosts, depending on the species and skeletal structures: intramembranous, perichondral and endochondral.[2] Of these, the latter two usually involve a cartilaginous template,[2] although vertebral bodies form through intramembranous ossification.[4] Hypertrophic chondrocytes have an important role in the final phases of higher vertebrates endochondral ossification, since they modify ECM, allowing matrix mineralization, vascular invasion and posterior bone formation.[6, 39] Similarly to other studies, hypertrophic chondrocytes were located proximal to the endplate,[4] although the most peripheral were embedded in a more basophilic matrix (HE) which corresponded with osteoid. Endochondral and perichondral ossification as well as chondral bone need further investigation in order to better understand the structural and chemical processes occurring in different fish species.[2] Moreover,

a chondroidal mechanism of ossification could be taking part in these processes, as suggested for Atlantic salmon and European seabass.[28, 49]

Concerns still exist on how to identify the specific pathogenic mechanisms involved in the onset of skeletal deformities, especially in anosteocytic bone fish. The histopathologic changes observed in fish with deformed and fused vertebrae further support the importance of identifying which cells are involved in the pathogenesis of vertebral problems. In mammals, osteocytes are believed to detect strain and mechanical load and to regulate cellular events implicated in the formation and remodeling of bone.[9, 39, 45] The fact that fish with anosteocytic bone may respond to loading conditions may indicate an alternative load detection mechanism.[9, 45] Some reports postulate that the osteoblasts and bone lining cells are likely candidates for sensing mechanical load in anosteocytic bone.[44, 45] The particular location of the cartilage in the growth zones may favor this hypothesis, although it requires further investigation. Moreover, other authors proposed that chondrocytes could serve as mechanosensors in most compressed areas.[5]

Studies with Atlantic salmon revealed an irregular and fragmented external elastic membrane in fish with fused and compressed vertebrae.[30, 50] The rupture of this membrane may be involved in the progression of spinal anomalies and likely co-evolves with other structural changes of the notochordal sheath.[50] In fact, the collagenous layer associated with the fragmented membrane was occasionally less evident or thinner. According to other studies, these lesions may decrease flexibility and possibly disturb nutritional transportation across the notochord, and could be related to the development of spinal fusions.[50]

In summary, the histological techniques complemented considerably the radiographic studies. Lesions consisted of alterations of the shape and orientation of bony trabeculae and vertebral endplates. The presence of chondrocytes in the endplates and within the IVS was a common response in different types of anomalies affecting teleost species with either osteocytic or anosteocytic bone. Some of the alterations in deformed vertebrae correspond with those seen in the initial stages of fusion, and in one case, with the aggravation of a primary fusion process. The cartilage proliferation from the growth zones into the IVS suggest that the chondrocyte mesenchymal origin could arise from metaplastic cells in the growth area, as a result of altered mechanical load. In later stages, the hyaline cartilage appears to be replaced by osseous tissue. Alterations in the external elastic membrane and the collagenous layer are presumably linked to vertebral deformities. Further work is needed to investigate the molecular pathways which may be involved in mechanosensor and local effector mechanisms, thus promoting the development of cartilage in anosteocytic bone anomalies.

Acknowledgements

References

1. Blanco-Vives B, Villamizar N, Ramos J, Bayarri MJ, Chereguini O, Sánchez-Vázquez FJ. Effect of daily thermo- and photo-cycles of different light spectrum on the development of Senegal sole (*Solea senegalensis*) larvae. *Aquaculture.* 2010;**306**:137-145.

2. Boglione C, Gavaia P, Koumoundouros G, et al. Skeletal anomalies in reared European fish larvae and juveniles. Part 1: normal and anomalous skeletogenic processes. *Reviews in Aquaculture.* 2013;**5**(Suppl 1):99-120.

3. Boglione C, Gisbert E, Gavaia P, et al. Skeletal anomalies in reared European fish larvae and juveniles. Part 2: main typologies, occurrences and causative factors. *Reviews in Aquaculture.* 2013;**5**(Suppl 1):121-167.

4. Cardeira J, Bensimon-Brito A, Pousão-Ferreira P, Cancela ML, Gavaia PJ. Lordotic-kyphotic vertebrae develop ectopic cartilage-like tissue in Senegalese sole (*Solea senegalensis*). *J Appl Ichthyol.* 2012;**28**:460-463.

5. Cardeira J, Mendes AC, Pousão-Ferreira P, Cancela ML, Gavaia PJ. Micro-anatomical characterization of vertebral curvatures in Senegalese sole *Solea senegalensis*. *J Fish Biol.* 2015;**86**:1796-1810.

6. Carlson CS, Weisbrode SE. Bone, joints, tendons and ligaments. In: McGavin MD, Zachary JF, eds. *Pathologic Basis of Veterinary Disease.* St Louis, USA: Mosby Elsevier; 2012:920-971.

7. de Azevedo AM, Losada AP, Barreiro A, Barreiro JD, Ferreiro I, Riaza A, Vázquez S, Quiroga MI. Skeletal anomalies in reared Senegalese sole *Solea senegalensis* juveniles: a radiographic approach. *Dis Aquat Org.* 2017;**124**:117-129.

8. de Azevedo AM, Losada AP, Ferreiro I, Riaza A, Vázquez S, Quiroga MI. New insight on vertebral anomalies in cultured Senegalese sole (*Solea senegalensis*, Kaup) at early stages of development. *J Fish Dis.* in press;doi: 10.1111/jfd.12575.

9. Dean MN, Shahar R. The structure-mechanics relationship and the response to load of the acellular bone of neoteleost fish: a review. *J Appl Ichthyol.* 2012;**28**:320-329.

10. Dionísio G, Campos C, Valente LMP, Conceição LEC, Cancela ML, Gavaia PJ. Effect of egg incubation temperature on the occurrence of skeletal deformities in *Solea senegalensis*. *J Appl Ichthyol.* 2012;**28**:471-476.

11. Epple M, Neues F. Synchrotron microcomputer tomography for the non-destructive visualization of the fish skeleton. *J Appl Ichthyol.* 2010;**26**:286-288.

12. FAO. Fisheries and aquaculture software. FishStatJ - software for fishery statistical time series [Global aquaculture production source 1950-2014]. *In: © FAO 2011-2016. FAO Fisheries and Aquaculture Department [online]. Rome: Updated on 21 July 2016. [Cited on 10 October 2016]. http://www.fao.org/fishery/statistics/software/fishstatj/en.*

13. Fernández I, Gisbert E. Senegalese sole bone tissue originated from chondral ossification is more sensitive than dermal bone to high vitamin A content in enriched *Artemia*. *J Appl Ichthyol.* 2010;**26**:344-349.

14. Fernández I, Hontoria F, Ortiz-Delgado JB, et al. Larval performance and skeletal deformities in farmed gilthead sea bream (*Sparus aurata*) fed with graded levels of vitamin A enriched rotifers (*Brachionus plicatilis*). *Aquaculture.* 2008;**283**:102-115.

15. Fernández I, Ortiz-Delgado JB, Sarasquete C, Gisbert E. Vitamin A effects on vertebral bone tissue homeostasis in gilthead sea bream (*Sparus aurata*) juveniles. *J Appl Ichthyol.* 2012;**28**:419-426.

16. Fernández I, Pimentel MS, Ortiz-Delgado JB, et al. Effect of dietary vitamin A on Senegalese sole (*Solea senegalensis*) skeletogenesis and larval quality. *Aquaculture.* 2009;**295**:250-265.

17. Fjelldal PG, Hansen T, Breck O, et al. Vertebral deformities in farmed Atlantic salmon (*Salmo salar* L.) - etiology and pathology. *J Appl Ichthyol.* 2012;**28**:433-440.

18. Fjelldal PG, Hansen TJ, Berg AE. A radiological study on the development of vertebral deformities in cultured Atlantic salmon (*Salmo salar* L.). *Aquaculture.* 2007;**273**:721-728.

19. Gavaia PJ, Dinis MT, Cancela ML. Osteological development and abnormalities of the vertebral column and caudal skeleton in larval and juvenile stages of hatchery-reared Senegal sole (*Solea senegalensis*). *Aquaculture.* 2002;**211**:305-323.

20. Gavaia PJ, Domingues S, Engrola S, et al. Comparing skeletal development of wild and hatchery-reared Senegalese sole (*Solea senegalensis*, Kaup 1858): evaluation in larval and postlarval stages. *Aquaculture Research.* 2009;**40**:1585-1593.

21. Gavaia PJ, Sarasquete C, Cancela ML. Detection of mineralized structures in early stages of development of marine Teleostei using a modified alcian blue-alizarin red double staining technique for bone and cartilage. *Biotechnic & Histochemistry: official publication of the Biological Stain Commission.* 2000;**75**:79-84.

22. Gorman KF, Handrigan GR, Jin G, Wallis R, Breden F. Structural and micro-anatomical changes in vertebrae associated with idiopathic-type spinal curvature in the curveback guppy model. *Scoliosis.* 2010;**5**:1-13.

23. Hall BK. *Bones and cartilage: developmental and evolutionary skeletal biology*. San Diego, USA: Academic Press; 2015.

24. Hjelde K, Bæverfjord G. Basic concepts of fish radiography. In: Bæverfjord G, Helland S, Hough C, eds. *Control of malformations in fish aquaculture: science and practice.* Liege, Belgium: Finefish. Federation of European Aquaculture Producers (FEAP); 2009:15-24.

25. Hough C. Improving the sustainability of European fish aquaculture by the control of malformations. Oral communication at the FINEFISH Final Workshop, 7 Sep 2009, held during Larvi 2009 - 5th Fish & Shellfish larviculture Symposium 7–10 Sep 2009, Ghent University, Belgium, 2009.

26. Howell B, Conceição L, Prickett R, Cañavate P, Mañanos E. Sole farming: nearly there but not quite? *Aquaculture Europe.* 2009;**34**:24-27.

27. Huysseune A. Chapter 18 - Skeletal system. In: Ostrander GK, ed. *The Laboratory Fish.* London, UK: Academic Press; 2000:307-317.

28. Kranenbarg S, van Cleynenbreugel T, Schipper H, van Leeuwen J. Adaptive bone formation in acellular vertebrae of sea bass (*Dicentrarchus labrax* L.). *J Exp Biol.* 2005;**208**:3493-3502.

29. Kranenbarg S, Waarsing JH, Muller M, Weinans H, van Leeuwen JL. Lordotic vertebrae in sea bass (*Dicentrarchus labrax* L.) are adapted to increased loads. *J Biomech.* 2005;**38**:1239-1246.

30. Kvellestad A, Høie S, Thorud K, Tørud B, Lyngøy A. Platyspondyly and shortness of vertebral column in farmed Atlantic salmon *Salmo salar* in Norway-description and interpretation of pathologic changes. *Dis Aquat Org.* 2000;**39**:97-108.

31. Losada AP. Combinación de técnicas radiológicas e histológicas para el estudio de las escoliosis en lenguado senegalés. Master Thesis. Universidade de Santiago de Compostela, Lugo, Spain; 2016.

32. Losada AP, de Azevedo AM, Barreiro A, et al. Skeletal malformations in Senegalese sole (*Solea senegalensis* Kaup, 1858): gross morphology and radiographic correlation. *J Appl Ichthyol.* 2014;**30**:804-808.

33. Ortiz-Delgado JB, Fernández I, Sarasquete C, Gisbert E. Normal and histopathological organization of the opercular bone and vertebrae in gilthead sea bream *Sparus aurata*. *Aquat Biol.* 2014;**21**:67-84.

34. Ortiz-Hidalgo C. Abelardo Gallego (1879–1930) and his contributions to histotechnology: The Gallego stains. *Acta Histochem.* 2011;**113**:189-193.

35. Pimentel MS, Faleiro F, Dionísio G, et al. Defective skeletogenesis and oversized otoliths in fish early stages in a changing ocean. *Journal of Experimental Biology.* 2014;**217**:2062-2070.

36. Ralis ZA, Watkins G. Modified tetrachrome method for osteoid and defectively mineralized bone in paraffin sections. *Biotech Histochem.* 1992;**67**:339-345.

37. Richard N, Fernandez I, Wulff T, et al. Dietary supplementation with vitamin K affects transcriptome and proteome of Senegalese sole, improving larval performance and quality. *Marine Biotechnology.* 2014;**16**:522-537.

38. Rodríguez JL, Peleteiro JB. *Cultivo del lenguado senegalés (Solea senegalensis)*. Madrid, Spain: Fundación Observatorio Español de Acuicultura; 2014.

39. Safadi FF, Barbe MF, Abdelmagid SM, et al. Bones structure, development and bone biology. In: Khurana SJ, ed. *Bone pathology.* New York, USA: Humana Press; 2009:1-50.

40. Sullivan M, Hammond G, Roberts RJ, Manchester NJ. Spinal deformation in commercially cultured Atlantic salmon, *Salmo salar* L.: a clinical and radiological study. *J Fish Dis.* 2007;**30**:745-752.

41. Witten PE, Gil-Martens L, Hall BK, Huysseune A, Obach A. Compressed vertebrae in Atlantic salmon *Salmo salar*: evidence for metaplastic

chondrogenesis as a skeletogenic response late in ontogeny. *Dis Aquat Org.* 2005;**64**:237-246.

42. Witten PE, Gil-Martens L, Huysseune A, Takle H, Hjelde K. Towards a classification and an understanding of developmental relationships of vertebral body malformations in Atlantic salmon (*Salmo salar* L.). *Aquaculture.* 2009;**295**:6-14.

43. Witten PE, Hall BK. Differentiation and growth of kype skeletal tissues in anadromous male Atlantic salmon (*Salmo salar*). *Int J Dev Biol.* 2002;**46**:719-730.

44. Witten PE, Hall BK. Teleost skeletal plasticity: modulation, adaptation, and remodelling. *Copeia.* 2015;**103**:727-739.

45. Witten PE, Huysseune A. A comparative view on mechanisms and functions of skeletal remodelling in teleost fish, with special emphasis on osteoclasts and their function. *Biological Reviews.* 2009;**84**:315-346.

46. Witten PE, Huysseune A. Mechanisms of chondrogenesis and osteogenesis in fins. In: Hall BK, ed. *Fins into limbs: evolution, development, and transformation.* Chicago, USA: The University of Chicago Press; 2007:79-92.

47. Witten PE, Obach A, Huysseune A, Baeverfjord G. Vertebrae fusion in Atlantic salmon (*Salmo salar*): development, aggravation and pathways of containment. *Aquaculture.* 2006;**258**:164-172.

48. Ytteborg E, Baeverfjord G, Torgersen J, Hjelde K, Takle H. Molecular pathology of vertebral deformities in hyperthermic Atlantic salmon (*Salmo salar*). *BMC Physiol.* 2010;**10**:12.

49. Ytteborg E, Torgersen J, Baeverfjord G, Takle H. Morphological and molecular characterization of developing vertebral fusions using a teleost model. *BMC Physiol.* 2010;**10**:13.

50. Ytteborg E, Torgersen JS, Pedersen ME, Baeverfjord G, Hannesson KO, Takle H. Remodeling of the notochord during development of vertebral fusions in Atlantic salmon (*Salmo salar*). *Cell Tissue Res.* 2010;**342**:363-376.

Figure legends

Figures 1-5. Control vertebrae, *Solea senegalensis*. **Figure 1.** Latero-lateral radiographic projection (LL) (a) and dorso-ventral radiographic projection (b) of the vertebral column showing vertebral alignment along the abdominal, caudal and caudal complex regions. **Figure 2.** LL detail of a vertebral segment revealing the internal bony structure of the vertebrae (dashed lines) and the intervertebral space (IVS) (asterisk). **Figure 3.** Histological section of a vertebral segment. Osseous tissue is arranged in bony trabeculae (arrow) and laminar bone in the endplates (arrowhead). The IVS (asterisk) is occupied by the notochordal structures. Note the denser central area of the IVS (star). Alcian blue/hematoxylin-eosin staining. **Figure 4.** Growth zone of the endplates showing a line of osteoblasts (black arrowhead) and the intervertebral connective tissue (white arrowhead). Note the lack of osteocytes in the endplate. Notochordal structures the IVS: central vacuolated chordocytes (star), the layer of chordoblasts (white arrow), the collagenous notochordal sheath (asterisk) and the external elastic membrane (black arrow) displaying an intense eosinophilic color. Hematoxylin-eosin. **Figure 5.** Vertebral segment displaying mature bone (bright red), in vertebral centra, and the blue stained endplates (arrowheads) revealing osteoid. Osteoid staining.

Figures 6-16. Deformed vertebrae, *Solea senegalensis*. **Figure 6.** Latero-lateral radiographic projection (LL) of deformed centra displaying flattened and radiodense endplates (white arrows) which were fused focally (white arrowhead). The intervertebral space (IVS) is narrower than the neighboring IVS. **Figure 7.** Histological evaluation of the same segment as Fig. 6. Altered and oblique

longitudinal trabeculae (black arrows) as a mirror-image, forming a convex structure. The endplates (white arrows) are asymmetric both in cranial-caudal axis as well as in dorsal-ventral axis. Note ventrally the presence of cartilaginous tissue in the proximity of the growth zone (rectangle). Hematoxylin-eosin (HE). **Figure 8.** Magnification of the area of the rectangle from Fig. 7. Cartilage nearby the growth zone (white arrowhead) and the endplates. Chondrocytes (black arrows) are evident in lacunae, surrounded by abundant cartilaginous extracellular matrix (ECM). HE. **Figure 9.** LL showing alterations of the vertebral internal structures as "K"-like vertebrae (dashed lines) and opposing flattened and radiodenser endplates (white arrows). The IVS is reduced and, in one point, the endplates fused with each other (white arrowhead). **Figure 10.** Section from the same segment as Fig. 9. Oblique longitudinal trabeculae (black arrows) and flattened endplate bone (white arrows) in facing vertebrae, showing protuberances of chondrocytes (asterisks) towards the narrower IVS. HE. Inset: Higher magnification of the area in the rectangle displaying one irregular protuberance formed by chondrocytes (black arrowhead) embedded in ECM. HE. **Figure 11.** Higher magnification of the ventral part of the intervertebral joint in Fig. 10. A deep blue matrix indicative of osteoid (white arrow) surrounded chondrocytes (thin black arrows) in the protuberances (asterisks), connecting both (black arrowhead). The notochord is sectioned in two parts (stars). Note the irregular external elastic membrane (white arrowhead) and the slightly thinner collagenous layer (thick black arrow). Osteoid staining. **Figure 12.** LL of a deformed vertebral segment. Alterations of the centra morphology, such as "K"-like shape (inversed "K" dashed lines) and both sides compression ("X" dashed lines) with flattened endplates. One vertebra (asterisk) is slightly enlarged compared to the normal vertebrae. A mild misalignment of the rachis towards the ventral aspect of the fish

(black arrow) was observed. **Figure 13.** Histopathologic section of the segment from Fig. 12. Cartilaginous tissue (asterisks) fills part of the IVS. Cartilage is symmetrically distributed, associated with the irregular endplates. The notochord condensed, occupying the remaining part of the IVS (stars). HE. **Figure 14.** High magnification of the areas (rectangle) shown in Fig. 13. Few chondrocytes (thin black arrows) in this zone, showing scarce amount of ECM around lacunae, as a halo. An eosinophilic matrix compatible with bone matrix (black arrowhead) surrounded these cells. Smaller chondrocytes (white arrow) and round lacunae (thick black arrow) are also observed. Note the fragmentation of the notochord external elastic membrane (white arrowheads). HE. **Figure 15.** LL of fused (black arrow) and deformed centra, displaying flattened and irregular endplates (white arrows). Centrum showing a "K"-like structure (dashed lines) as well as a mild enlargement respect to the adjacent caudal vertebra (asterisk). Fused vertebrae are also shorter in the cranial-caudal axis. The IVS between fused and deformed centra is narrow. **Figure 16.** Histological section of the same sample of Fig. 15. (a) Fused vertebrae displaying reorganized trabeculae. The line of fusion is merged to longitudinal trabeculae (black arrowhead). Adjacent vertebra also shows deformation with alterations of longitudinal trabeculae (black arrow). The IVS is completely filled with cartilage (asterisk) and surrounded by flattened and irregular endplates (white arrows). HE. (b) The notochordal structures (star) occupied the IVS. A matrix compatible with ECM was observed in a small area (asterisk). Alcian blue/periodic acid-Schiff staining (AB-PAS). Inset: Magnification of the rectangle area. Remnants of chondrocytes (black arrows) surrounded by alcian blue stained ECM (asterisk) in the vertebral fusion center. AB-PAS.

Figures 17-19. Detailed view of the intervertebral space (IVS) area from Fig. 13, *Solea senegalensis*. **Figure 17.** Cartilage is proliferating from the growth zone (white arrowhead) towards the IVS (asterisk). The tissue is distributed in a central area (C) with small elongated chondrocytes, at both sides (H) the hypertrophied cartilaginous cells (black arrows) and the area close to the endplates (A). A purple stained cartilaginous extracellular matrix (ECM) surrounds the chondrocytes and shows a darker color in the area in contact with the endplates (A). Note the irregular external elastic membrane (black arrowhead) and the thinner collagenous sheath (white arrow). Hematoxylin-eosin. **Figure 18.** Chondrocytes embedded in an abundant alcian blue stained ECM (white arrow), especially in the central area (C). Note the slight change in the matrix color around the hypertrophic chondrocytes (thin black arrows) in the intermediate zone (H) to pink (white arrowhead). In the area near the endplate bone (A), the ECM (black thick arrow) appears blue stained although the interterritorial matrix (star) has almost the same color as the adjacent bone. Some trabecular lacunae are located in the endplates near areas with chondrocytes (black arrowhead). Alcian blue/periodic acid-Schiff staining. **Figure 19.** The cartilaginous tissue is adjacent to the endplate bone near the growth zone (A). Chondrocytes in this area (black arrows) are embedded in a deep blue osteoid matrix (star). In the furthest parts of the endplate, a pale blue cartilaginous ECM is present around the chondrocytes (white arrows) and in the IVS (asterisk). Note the presence of a considerable number of blood capillaries (black arrowheads) in the growth zone. Osteoid staining.

Figures 20-21. Schematic illustration of the common histological changes. **Figure 20.** Control vertebrae. 1. Longitudinal trabeculae. 2. Concave endplates. 3. Trabecula

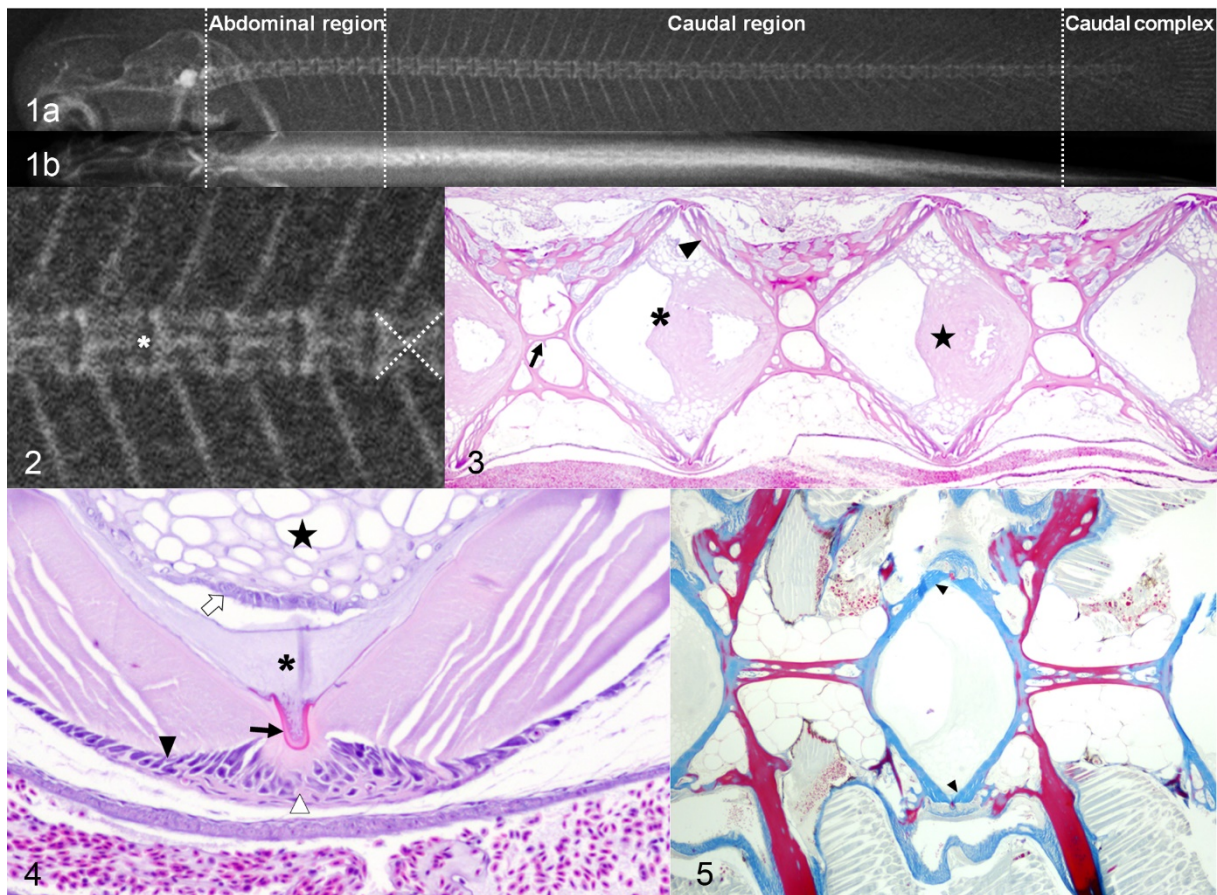lacunae. 4. Osteoblasts layer. 5. Chordocytes. 6. Layer of chordoblasts. 7. Collagenous notochordal sheath. 8.External elastic membrane. 9. Connective tissue.

Figure 21. Deformed vertebrae. 1. Symmetrical alterations of the bony longitudinal trabeculae. 2. Reduced concavity and irregular endplates. 3. Chondrocytes located in the endplates, occasionally forming protuberances towards the notochord (asterisk) in the intervertebral space (IVS) in facing vertebrae. 4. Isolated chondrocytes embedded in a bone matrix. 5. Proliferation of cartilaginous tissue invading the IVS showing some organization: central area (C) with small chondrocytes; hypertrophied chondrocytes (H) and chondrocytes associated with the endplate (A) showing the presence of some trabecula lacunae (arrowheads). 6. Scattered and irregular external elastic membrane. 7. Thinner collagenous layer. 8. High number of blood capillaries in the connective tissue near the growth zone. 9. Unaffected area.

Figures 22-25: Fused vertebrae, *Solea senegalensis*. **Figure 22.** Latero-lateral radiographic projection (LL) of a complete fusion between two vertebrae (dashed line) exhibiting two neural and haemal elements (white arrowheads). The union is reshaped although the line of fusion remains (white arrow) between the shortened vertebral bodies. **Figure 23.** Histologic view of the same vertebral segment as Fig. 22. (a) Bone internal longitudinal trabeculae from both centra are reoriented and connected in the cranio-caudal direction. In the middle point, the perpendicular line of fusion remained (white arrow). Hematoxylin-eosin (HE). Inset: Higher magnification of the area in the rectangle. A remnant of the notochordal structures (star) persisted in the intersection of the trabeculae. Note the presence of the eosinophilic external elastic membrane (black arrow). HE. (b) Mature osseous tissue is present in the reorganized trabeculae of the fused centra and the fusion line (black arrow). The endplates display the deep blue color of osteoid (black arrowhead). Osteoid staining.
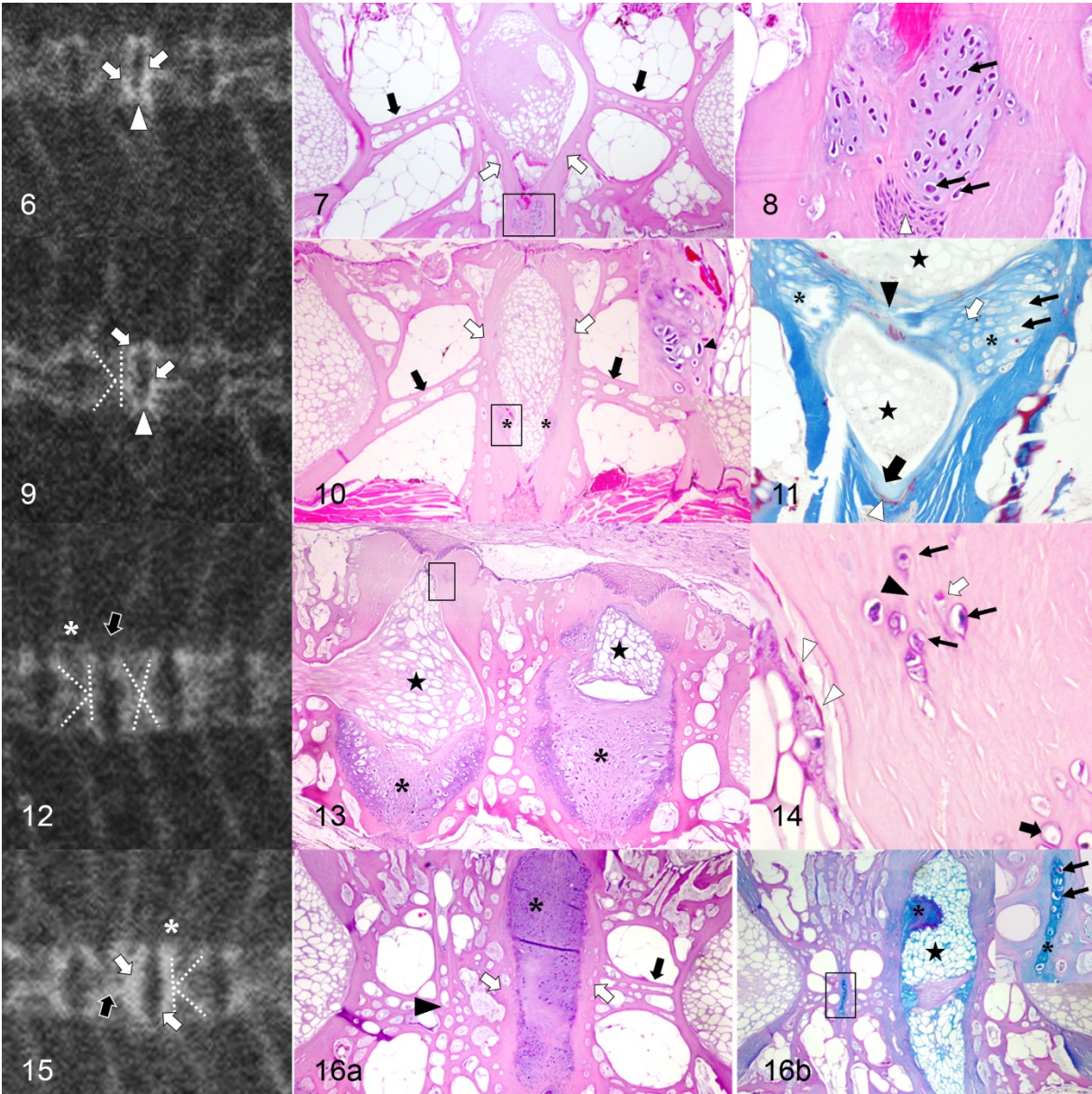
Figure 24. LL of a specimen showing the fusion of three vertebral centra (dashed line) in the abdominal region. The correspondent neural spines are visible (white arrowheads). **Figure 25.** Histological view of the same area of Fig. 24. The vertebral trabeculae were almost reorganized. Perpendicular osseous trabeculae, resembling the fusion lines, were present (white arrows). Two ovoid areas contain notochordal structures (black arrowheads). Alcian blue/hematoxylin-eosin staining

Figures

Figures 1-5. Control vertebrae, *Solea senegalensis*. **Figure 1.** Latero-lateral radiographic projection (LL) (a) and dorso-ventral radiographic projection (b) of the vertebral column showing vertebral alignment along the abdominal, caudal and caudal complex regions. **Figure 2.** LL detail of a vertebral segment revealing the internal bony structure of the vertebrae (dashed lines) and the intervertebral space (IVS) (asterisk). **Figure 3.** Histological section of a vertebral segment. Osseous tissue is arranged in bony trabeculae (arrow) and laminar bone in the endplates (arrowhead). The IVS (asterisk) is occupied by the notochordal structures. Note the denser central area of the IVS (star). Alcian blue/hematoxylin-eosin staining. **Figure 4.** Growth zone of the endplates showing a line of osteoblasts (black arrowhead) and the intervertebral connective tissue (white arrowhead). Note the lack of osteocytes in
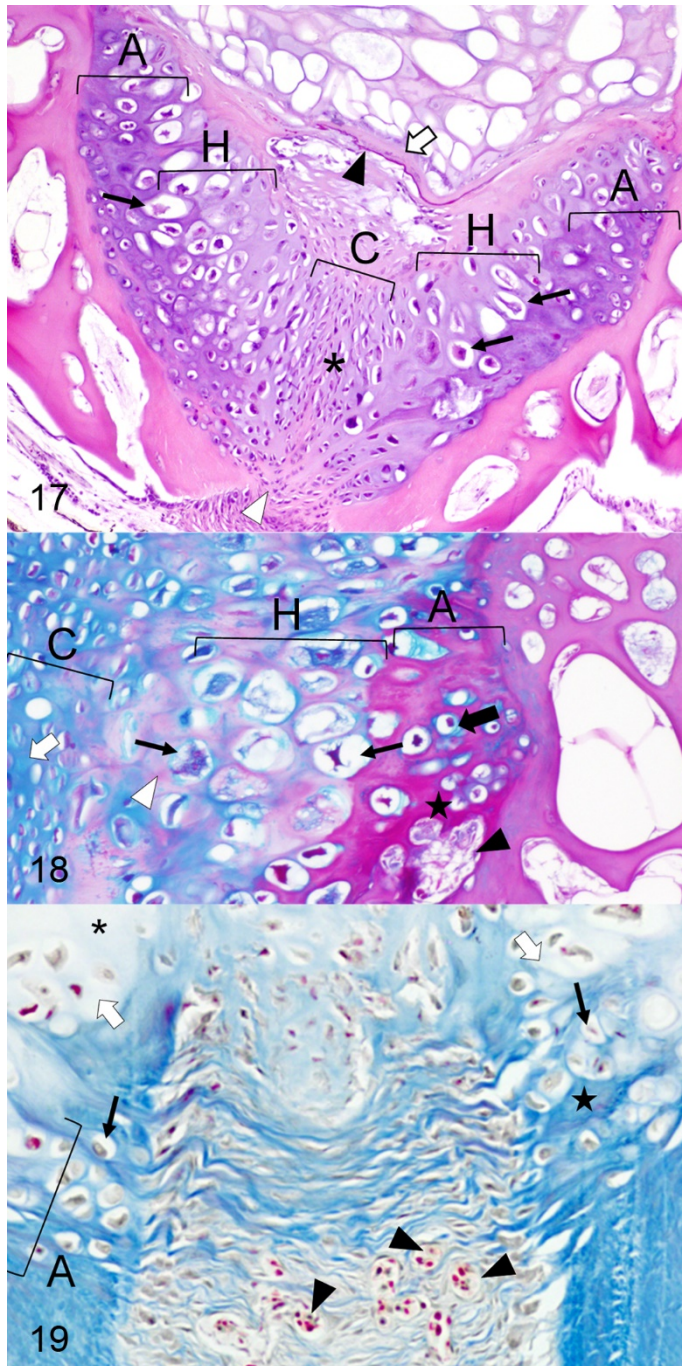
the endplate. Notochordal structures the IVS: central vacuolated chordocytes (star), the layer of chordoblasts (white arrow), the collagenous notochordal sheath (asterisk) and the external elastic membrane (black arrow) displaying an intense eosinophilic color. Hematoxylin-eosin. **Figure 5.** Vertebral segment displaying mature bone (bright red), in vertebral centra, and the blue stained endplates (arrowheads) revealing osteoid. Osteoid staining.

Figures 6-16. Deformed vertebrae, *Solea senegalensis*. **Figure 6.** Latero-lateral radiographic projection (LL) of deformed centra displaying flattened and radiodense endplates (white arrows) which were fused focally (white arrowhead). The intervertebral space (IVS) is narrower than the neighboring IVS. **Figure 7.** Histological evaluation of the same segment as Fig. 6. Altered and oblique longitudinal trabeculae (black arrows) as a mirror-image, forming a convex structure. The endplates (white arrows) are asymmetric both in cranial-caudal axis as well as in dorsal-ventral axis. Note ventrally the presence of cartilaginous tissue in the proximity of the growth zone (rectangle). Hematoxylin-eosin (HE). **Figure 8.** Magnification of the area of the rectangle from Fig. 7. Cartilage nearby the growth zone (white arrowhead) and the endplates. Chondrocytes (black arrows) are evident in lacunae, surrounded by abundant cartilaginous extracellular matrix (ECM). HE. **Figure 9.** LL showing alterations of the vertebral internal structures as "K"-like vertebrae (dashed lines) and opposing flattened and radiodenser endplates (white arrows). The IVS is reduced and, in one point, the endplates fused with each other (white arrowhead). **Figure 10.** Section from the same segment as Fig. 9. Oblique longitudinal trabeculae (black arrows) and flattened endplate bone (white arrows) in facing vertebrae, showing protuberances of chondrocytes (asterisks) towards the narrower IVS. HE. Inset: Higher magnification of the area in the rectangle displaying one irregular protuberance formed by chondrocytes (black arrowhead) embedded in ECM. HE. **Figure 11.** Higher magnification of the ventral part of the intervertebral joint in Fig. 10. A deep blue matrix indicative of osteoid (white arrow) surrounded chondrocytes (thin black arrows) in the protuberances (asterisks), connecting both (black arrowhead). The notochord is sectioned in two parts (stars). Note the irregular external elastic membrane (white arrowhead) and the slightly thinner collagenous
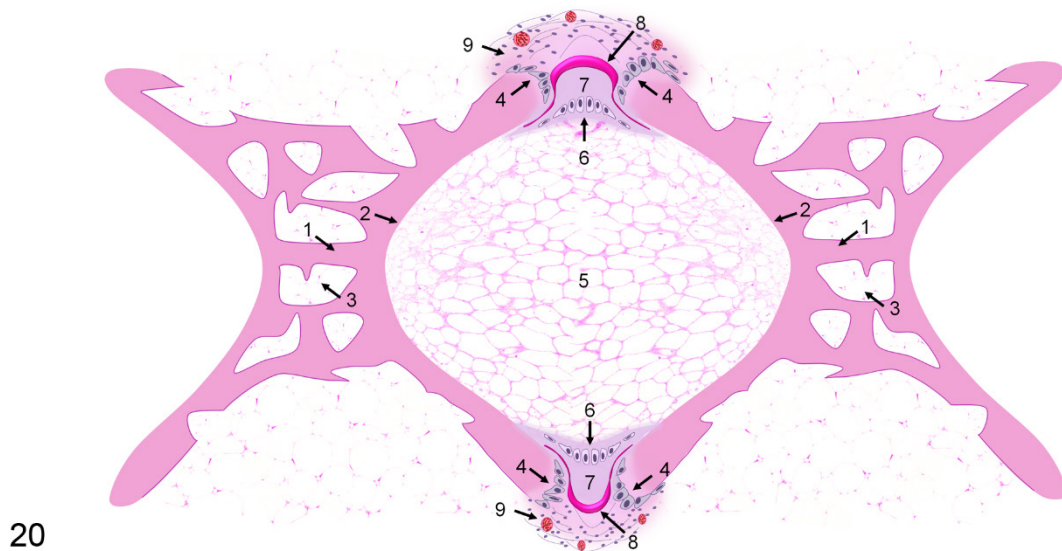
layer (thick black arrow). Osteoid staining. **Figure 12.** LL of a deformed vertebral segment. Alterations of the centra morphology, such as "K"-like shape (inversed "K" dashed lines) and both sides compression ("X" dashed lines) with flattened endplates. One vertebra (asterisk) is slightly enlarged compared to the normal vertebrae. A mild misalignment of the rachis towards the ventral aspect of the fish (black arrow) was observed. **Figure 13.** Histopathologic section of the segment from Fig. 12. Cartilaginous tissue (asterisks) fills part of the IVS. Cartilage is symmetrically distributed, associated with the irregular endplates. The notochord condensed, occupying the remaining part of the IVS (stars). HE. **Figure 14.** High magnification of the areas (rectangle) shown in Fig. 13. Few chondrocytes (thin black arrows) in this zone, showing scarce amount of ECM around lacunae, as a halo. An eosinophilic matrix compatible with bone matrix (black arrowhead) surrounded these cells. Smaller chondrocytes (white arrow) and round lacunae (thick black arrow) are also observed. Note the fragmentation of the notochord external elastic membrane (white arrowheads). HE. **Figure 15.** LL of fused (black arrow) and deformed centra, displaying flattened and irregular endplates (white arrows). Centrum showing a "K"-like structure (dashed lines) as well as a mild enlargement respect to the adjacent caudal vertebra (asterisk). Fused vertebrae are also shorter in the cranial-caudal axis. The IVS between fused and deformed centra is narrow. **Figure 16.** Histological section of the same sample of Fig. 15. (a) Fused vertebrae displaying reorganized trabeculae. The line of fusion is merged to longitudinal trabeculae (black arrowhead). Adjacent vertebra also shows deformation with alterations of longitudinal trabeculae (black arrow). The IVS is completely filled with cartilage (asterisk) and surrounded by flattened and irregular endplates (white arrows). HE. (b) The notochordal structures (star) occupied the IVS. A matrix compatible with ECM was observed in a small area

(asterisk). Alcian blue/periodic acid-Schiff staining (AB-PAS). Inset: Magnification of the rectangle area. Remnants of chondrocytes (black arrows) surrounded by alcian blue stained ECM (asterisk) in the vertebral fusion center. AB-PAS.
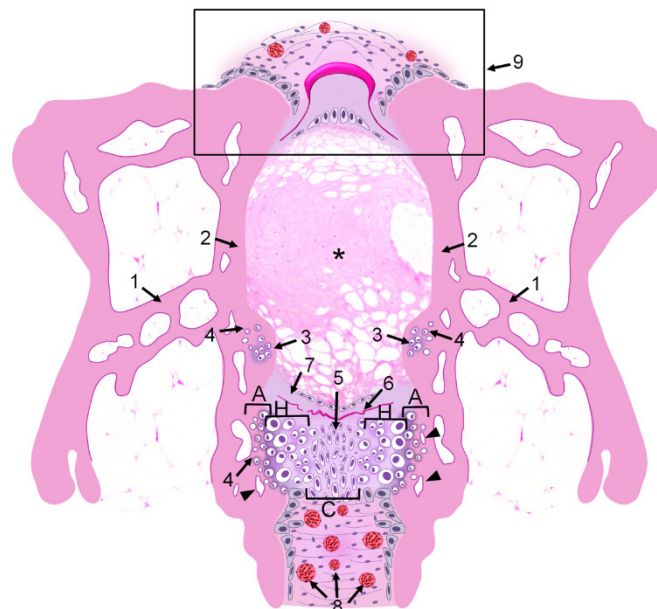

Figures 17-19. Detailed view of the intervertebral space (IVS) area from Fig. 13, *Solea senegalensis*. **Figure 17.** Cartilage is proliferating from the growth zone (white arrowhead) towards the IVS (asterisk). The tissue is distributed in a central area (C)

with small elongated chondrocytes, at both sides (H) the hypertrophied cartilaginous cells (black arrows) and the area close to the endplates (A). A purple stained cartilaginous extracellular matrix (ECM) surrounds the chondrocytes and shows a darker color in the area in contact with the endplates (A). Note the irregular external elastic membrane (black arrowhead) and the thinner collagenous sheath (white arrow). Hematoxylin-eosin. **Figure 18.** Chondrocytes embedded in an abundant alcian blue stained ECM (white arrow), especially in the central area (C). Note the slight change in the matrix color around the hypertrophic chondrocytes (thin black arrows) in the intermediate zone (H) to pink (white arrowhead). In the area near the endplate bone (A), the ECM (black thick arrow) appears blue stained although the interterritorial matrix (star) has almost the same color as the adjacent bone. Some trabecular lacunae are located in the endplates near areas with chondrocytes (black arrowhead). Alcian blue/periodic acid-Schiff staining. **Figure 19.** The cartilaginous tissue is adjacent to the endplate bone near the growth zone (A). Chondrocytes in this area (black arrows) are embedded in a deep blue osteoid matrix (star). In the furthest parts of the endplate, a pale blue cartilaginous ECM is present around the chondrocytes (white arrows) and in the IVS (asterisk). Note the presence of a considerable number of blood capillaries (black arrowheads) in the growth zone. Osteoid staining.
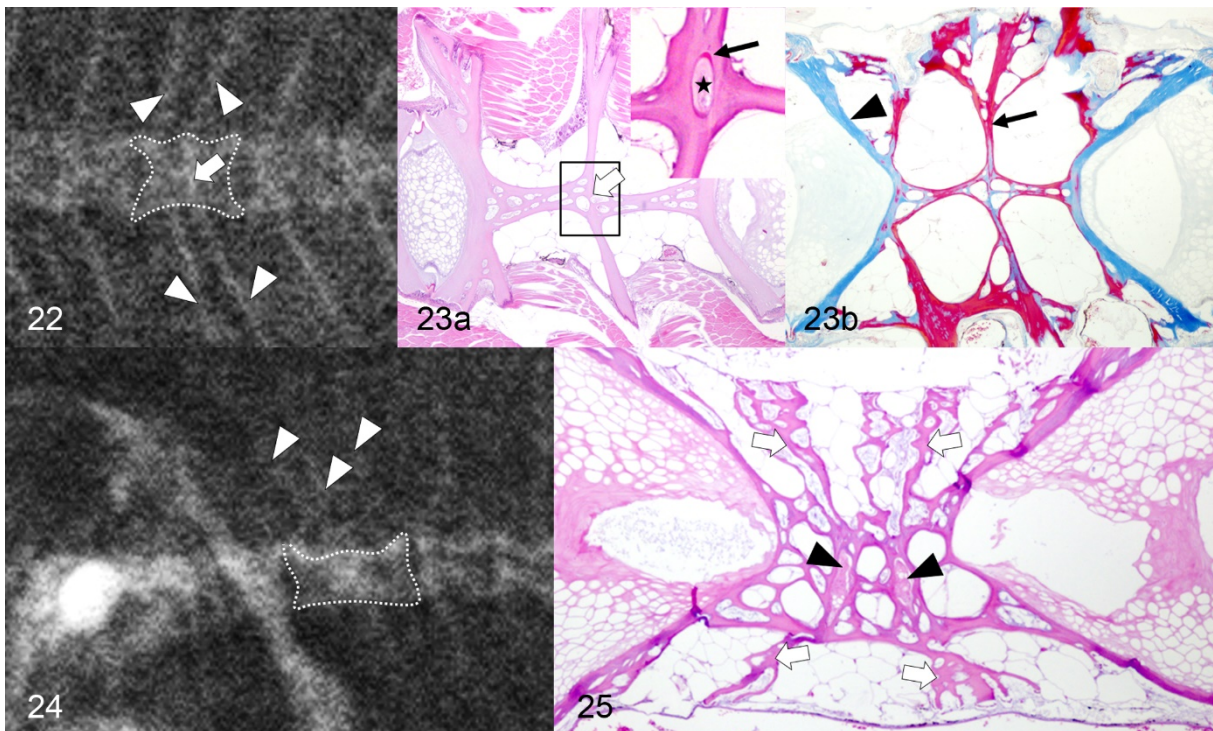
20

21

Figures 20-21. Schematic illustration of the common histological changes. **Figure 20.** Control vertebrae. 1. Longitudinal trabeculae. 2. Concave endplates. 3. Trabecula lacunae. 4. Osteoblasts layer. 5. Chordocytes. 6. Layer of chordoblasts. 7. Collagenous notochordal sheath. 8.External elastic membrane. 9. Connective tissue. **Figure 21.** Deformed vertebrae. 1. Symmetrical alterations of the bony longitudinal trabeculae. 2. Reduced concavity and irregular endplates. 3. Chondrocytes located in the endplates, occasionally forming protuberances towards the notochord (asterisk) in the intervertebral space (IVS) in facing vertebrae. 4. Isolated chondrocytes

embedded in a bone matrix. 5. Proliferation of cartilaginous tissue invading the IVS showing some organization: central area (C) with small chondrocytes; hypertrophied chondrocytes (H) and chondrocytes associated with the endplate (A) showing the presence of some trabecula lacunae (arrowheads). 6. Scattered and irregular external elastic membrane. 7. Thinner collagenous layer. 8. High number of blood capillaries in the connective tissue near the growth zone. 9. Unaffected area.

Figures 22-25: Fused vertebrae, *Solea senegalensis*. **Figure 22.** Latero-lateral radiographic projection (LL) of a complete fusion between two vertebrae (dashed line) exhibiting two neural and haemal elements (white arrowheads). The union is reshaped although the line of fusion remains (white arrow) between the shortened vertebral bodies. **Figure 23.** Histologic view of the same vertebral segment as Fig. 22. (a) Bone internal longitudinal trabeculae from both centra are reoriented and connected in the cranio-caudal direction. In the middle point, the perpendicular line of fusion remained (white arrow). Hematoxylin-eosin (HE). Inset: Higher magnification

of the area in the rectangle. A remnant of the notochordal structures (star) persisted in the intersection of the trabeculae. Note the presence of the eosinophilic external elastic membrane (black arrow). HE. (b) Mature osseous tissue is present in the reorganized trabeculae of the fused centra and the fusion line (black arrow). The endplates display the deep blue color of osteoid (black arrowhead). Osteoid staining.

Figure 24. LL of a specimen showing the fusion of three vertebral centra (dashed line) in the abdominal region. The correspondent neural spines are visible (white arrowheads). **Figure 25.** Histological view of the same area of Fig. 24. The vertebral trabeculae were almost reorganized. Perpendicular osseous trabeculae, resembling the fusion lines, were present (white arrows). Two ovoid areas contain notochordal structures (black arrowheads). Alcian blue/hematoxylin-eosin staining.